NATO ASI

1, 743 (1992)
"Clusters to Crystals"
ed by Dormann & Fiorani
(Elsevier, Amsterdam)

MAGNETISM OF SMALL PARTICLES

S. GANGOPADHYAY, L. YIPING and G. C. HADJIPANAYIS
Department of Physics, University of Delaware, Newark, Delaware 19716.

C. M. SORENSEN and K. J. KLABUNDE*
*Department Of Physics, *Department Of Chemistry, Kansas State University, Manhattan, Kansas 66506.*

V. PAPAEFTHYMIOU and A. KOSTIKAS*
Department of Physics, University of Ioannina, Greece.
**Institute of Material-Science, NCSR Demokritos, Athens, Greece.*

ABSTRACT. The magnetic and structural properties of fine Fe particles and Fe-B particles prepared by vapor deposition and $NaBH_4$ reduction respectively, have been studied. Fe particles in the range of 50-300 Å were obtained by varying the argon pressure during evaporation in the range of 0.5-30 torr. The Fe-B powders were prepared by reducing $FeCl_3$ with $NaBH_4$ in aqueous solution. Particle sizes in the range of 300-600 Å were obtained. The X-ray patterns indicate that powders with B content higher than 20 % are amorphous and those with lower than 20 % are crystalline. The dependence of magnetization and coercivity on particle size and temperature have been studied, using SQUID magnetometry and Mössbauer spectroscopy. The magnetic and structural data suggest a core/shell type of structure, where the core consists of metallic Fe (and/or Fe-B) and the shell is composed of Fe-oxides. The values of coercivity obtained (1200 Oe) are two orders of magnitude higher than those in bulk Fe and Fe-B metallic glasses.

1. Introduction

Metals and alloys in the nanocrystalline form exhibit properties which are drastically different from the bulk. This opens up an area of research for nano-structured materials that is very challenging scientifically and technologically. Fine particles are widely used for magnetic recording media, ferro-fluids, catalysts, medical diagnostics, drug delivery systems and pigments in paints and ceramics [1-3]. Enhanced magnetic properties of fine ferromagnetic particles make them very promising candidates for high density magnetic recording media.

Fine Fe particles (~ 200 Å) have been reported to have coercivities as high as two orders of magnitude higher than bulk Fe and their saturation magnetization can be varied between 20 - 90 % (of the bulk value) depending on particle size [4]. Particles in their fine form (few 100's of Å) are very pyrophoric and hence require a controlled surface passivation. The magnetic properties of the particles are strongly dependent on the form and constituents of the surface layers which constitute a major volume fraction in ultra-fine particles (UFPs). Thus a greater understanding and control of the surface layer in UFPs would result in optimum magnetic properties.

Ultrafine transition metal boron particles can be synthesized by reduction of metal salts with $NaBH_4$ in aqueous solution. A number of studies have dealt with the magnetic and structural properties of these fine particles [5-7]. The chemical reduction technique is very easy to use and it is very important scientifically and technologically. So far this technique has been used as granted to prepare boron containing particles. Very few studies if any exist to study the chemistry of the process. Our group is presently studying the detailed chemistry of the reduction process as it progresses to form the final product, in order to be able to get a better control over the latter part.

In this paper we will briefly review our recent studies on the structural and magnetic properties of fine Fe and Fe-B particles made by vapor deposition and $NaBH_4$ reduction technique, respectively. The size and temperature dependence of magnetic properties have been studied. A shell/core model [8] has been used to explain the magnetic properties and their temperature dependence.

2. Experimental

2.1. VAPOR DEPOSITION

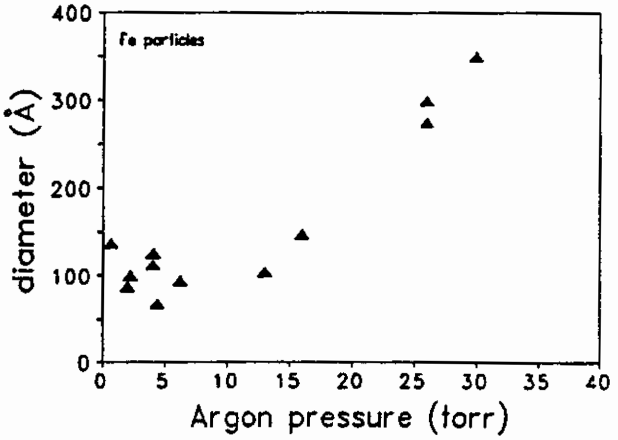

Figure 1. The particle size increases as the argon pressure during the evaporation increases.

In the vapor deposition technique the material is evaporated in the presence of an inert gas. The metal vapor condenses due to collisions with the inert gas molecules to form clusters of atoms which subsequently grow to form particles. These particles then agglomerate together to form chains/dendrites as they travel towards a cold substrate, due to gas convection currents and thermophoresis. The resulting sample is in the form of black soot or "smoke", which can be easily scraped off the substrate using a glass slide.The particles formed by the condensation technique are very pure and clean chemically. The particle size can be effectively controlled by various means including, the molecular weight of the inert gas, evaporation source temperature, inert gas pressure and the substrate temperature.

The joule heating element used in this study was an alumina-coated tungsten crucible. The distance between the crucible and the water cooled Cu substrate was optimized in order to maximize the yield. Argon gas was used to provide the inert atmosphere during evaporation. The dynamic pressure of argon used during evaporation varied between 1 and 30 torr. The particles obtained were of the size of 50-300 Å. The increase in particle diameter as the gas pressure increased is shown in Figure 1. With increasing gas pressure the mean free path of metal vapor is decreased, because of more collisions, leading to formation of larger particles.

The metal particles made by this technique are highly pyrophoric and require surface passivation which, as it will be shown later, plays an important role in the magnetic behavior of the whole particle. An argon-air mixture was introduced into the chamber for this purpose after evaporation of particles (volume ratio of argon to O_2 being about 300). The extent of oxidation could be varied by carefully changing the O_2 to argon ratio in the chamber after the evaporation. Samples with virtually no oxide could be prepared by sandwiching the metal particles between two thin films of Ag, with the whole assembly deposited on a Kapton substrate.

2.2. $NaBH_4$ REDUCTION

Powdered Fe-B samples were prepared by reducing aqueous solutions of iron salts with $NaBH_4$. The composition and structure of the powders were found to depend on the method of sample preparation. Crystalline Fe-B particles can be prepared using a "Y junction" through which aqueous solutions of $FeCl_3$ and $NaBH_4$ are mixed in the presence of an external magnetic field of 1 kOe. The maximum amount of boron that was found in the Fe-B powders was only 15 at% when the "Y junction" technique was used. However, if the $NaBH_4$ solution is added into a well stirred iron salt solution, a high boron-content powder is obtained which is also found to be amorphous (approximately 40 at% B). The black precipitates were separated and repeatedly washed with distilled water and subsequently in acetone, and then dried in a N_2 atmosphere chamber.

3. Magnetic and structural properties

3.1. VAPOR DEPOSITION

The enhanced and interesting magnetic properties of nanostructured materials are due to finite size effects, which makes the study of structure morphology and microstructure very crucial. Particles size and morphology in this study was determined using a transmission electron microscope. Different areas in the bright field micrographs were enlarged and sampled to arrive at the median particle size. Particle size distribution was found to follow a log-normal distribution. Small particles were more uniform in their size distribution ascompared to the bigger particle samples.

Particles formed were roughly spherical in the case of Fe and Co. Small deviations from sphericity were observed as the particle size increased. In the case of Ni particles, however, complete sphericity was observed up to about 150 Å. In most of the particles the observed images showed a distinct contrast with the center of particle being darker than its periphery. This could be due to the presence of an oxide shell around a metallic core brought in by the intentional passivation. The core/shell structure was also evident from dark field micrographs. A typical transmission electron micrograph (TEM) of an Fe sample is shown in Figure 2.

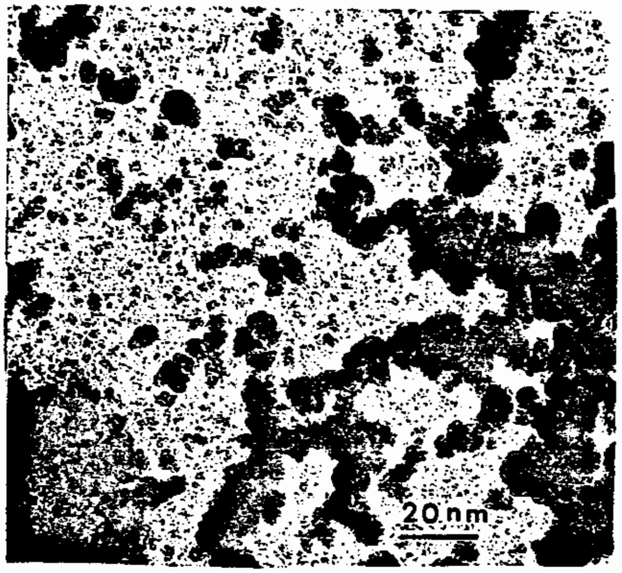

Figure 2. Bright field micrograph of fine Fe particles with a median particle size of 113 Å.

The sharpness of the metal diffraction lines in both X-ray and selected area diffraction patterns increased as the particle size increased. The lines due to the oxides were always broad and diffuse, which could be due either to their amorphous or poly-crystalline form. The oxides found in the case of Fe particles were Fe_3O_4 and/or γ-Fe_2O_3. CoO and NiO were found in the case of Co and Ni, respectively. X-ray photoelectron spectroscopy (XPS) was also used to determine the type of oxides. The amount of Fe_3O_4 was always found to be much higher than γ-Fe_2O_3.

Saturation magnetization as a function of particle diameter is shown in Figure 3. In the case of Fe particles the magnetization values varied between 25 and 190 emu/g as the particle size increased from 60 to 200 Å, respectively. The general decrease of magnetization with decreasing particle diameter can be attributed to the increased volume fraction of oxides in smaller particles. The reduction of magnetization below the oxide value will be discussed in section 4.

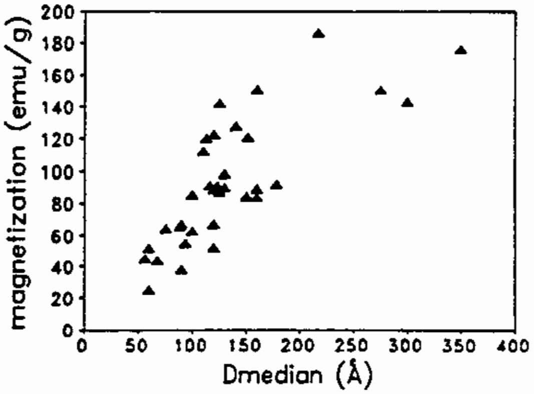

Figure 3. Size dependence of saturation magnetization at 10 K.

Coercivity as function of size is shown in Figure 4 at room temperature. The smaller particles are superparamagnetic even below room temperature. The particle size obtained in Fe particles was always below the single domain size, hence an increase in coercivity (due to thermal effects) with particle size was observed [9]. Temperature dependence of coercivity for different particle sizes is shown in Figure 5. The main feature of this graph is the crossover temperature at about 40 K, where the particles show an opposite size dependence of coercivity above and below this temperature.

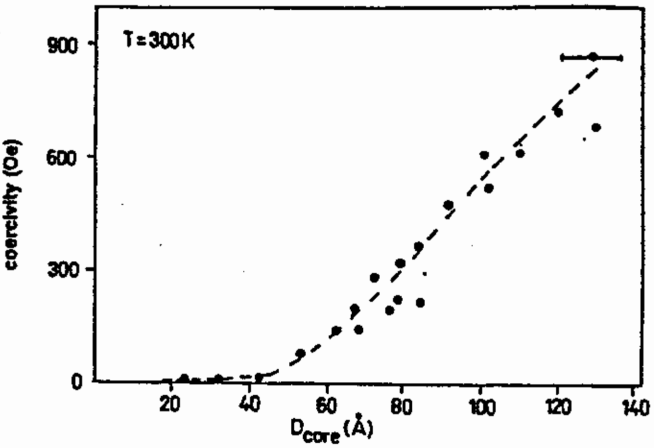

Figure 4. Size dependence of coercivity for Fe particles at room temperature. Particles below 40 Å core diameter show superparamagnetism.

The high field magnetization data were fit to the law of approach to saturation [10], to determine the anisotropy constant K using the expression

$$M=M_s[1-A/H-B/H^2-C/H^3]+\chi H \qquad (1)$$

where the first term (A/H) is related to the magnetization process in lower fields. The coefficients B and C are functions of the magnetocrystalline anisotropy constant K_1 and saturation magnetization M_s and χ is the high field susceptibility. Furthermore, the H_c vs $T^{1/2}$ law [9] was also used to estimate the value of "K". Both of these techniques gave values of K of the order of 10^6 ergs/cc, which is an order of magnitude higher than the bulk anisotropy value for Fe (4.8 x 10^5 ergs/cc).

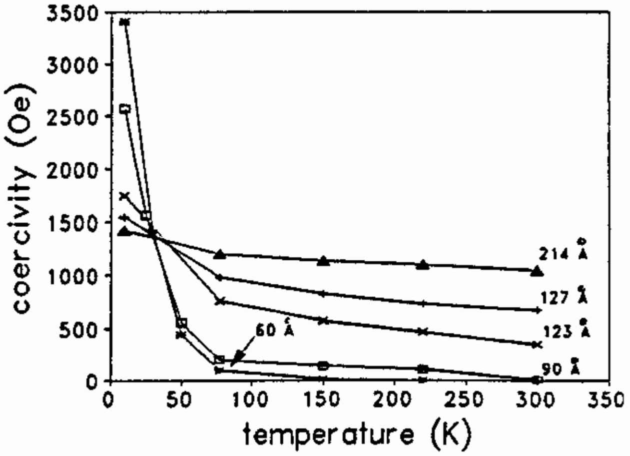

Figure 5. Temperature dependence of coercivity for Fe particles with different size. Note the crossover temperature of curves at about 30 - 40 K.

Mössbauer spectra on fine Fe particles [11] with median diameter 114 Å are shown in Figure 6. The spectra at the three temperatures are characteristic of mixtures of α-Fe with its oxides Fe_3O_4 and/or γ-Fe_2O_3. The presence of the sharp sextet as the temperature increases from 4.2 to 300 K indicates the ferromagnetic nature of α-Fe. However the oxide spectra evolve from a magnetically split spectrum to a very broad quadrupole doublet as the temperature increases from 85 to 300 K. This broadness of the oxide spectra at room temperature indicates that there exists a magnetic interaction between the superparamagnetic oxide shell and the ferromagnetic Fe core [12].

3.2. $NaBH_4$ REDUCTION

Figure 7 shows the x-ray diffraction patterns for Fe-B powders with different boron concentrations. When the boron content is higher than 20 at%, the powders were found to be amorphous; otherwise they were crystalline with a bcc structure and with slightly broad peaks due to particle size effects. The particle size as determined from the TEM micrograph is found to be in the range of 300-600 Å in all the powders. Figures 8 and 9 show the magnetization and coercivity as a function of boron concentration. M_s is found to decrease initially with B content, going through a minimum at 15 at% and then increase again for higher B content. The largest change in magnetization was observed in the smallest particles. M_s is expected to decrease with increasing B content and it is usually lower in amorphous samples than in crystalline samples [13]. The large difference between the values of the M_s for the smaller and larger particles may be explained by oxidation effects. Smaller particles have a higher surface to volume ratio than larger particles and as a result smaller particles get more oxidized. When the B content is higher than 20 at%, the particles become amorphous and the particles do not oxidize as much as in the crystalline state and therefore M_s is higher. The coercivity was

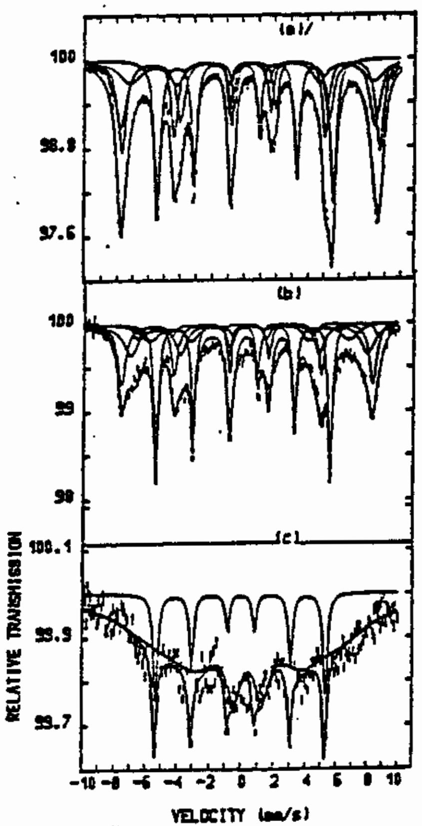

Figure 6. Mössbauer spectra of a 114 Å sized Fe sample at: (a) 4.2 K (b) 85 K (c) 300 K

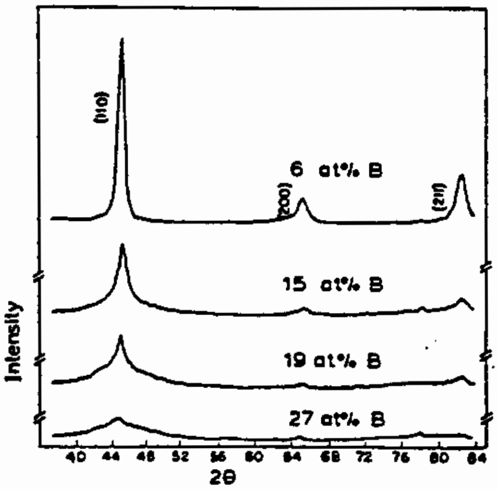

Figure 7. X-ray diffraction pattern for different B content, in Fe-B particles.

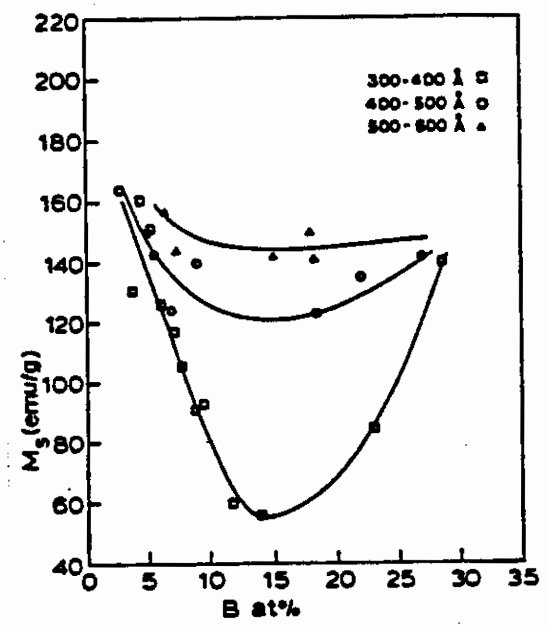

Figure 8. M_s as a function of B content for FeB particles.

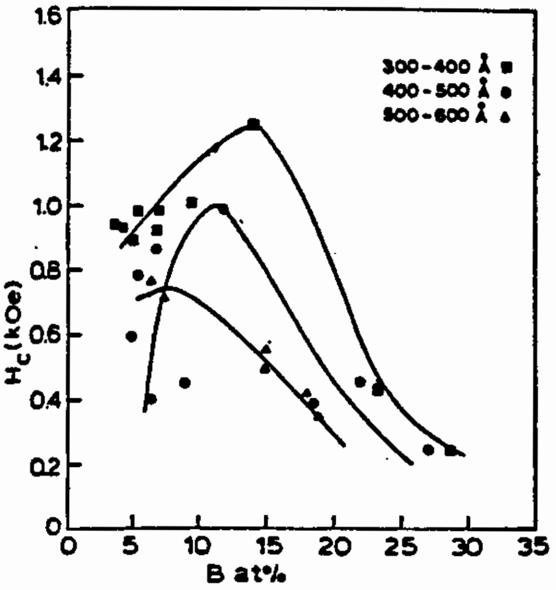

Figure 9. Coercivity as function of B content in FeB particles.

found to increase with decreasing B concentration and go through a maximum at a B content 15 at%. The large scattering of data is due to the uncertainty of size determination and to various degrees of oxidation. The coercivity obtained in fine Fe-B particles is at least two orders of magnitude higher than that reported on metallic glasses. It is worth to note, however, that the highest H_c was obtained in samples with a higher oxide content. This was confirmed by Mössbauer spectroscopy. The decrease of coercivity with decreasing particle size may be due to the multidomain nature of the larger particles.

Typical spectra obtained at 85 K for the amorphous and crystalline samples are shown in Figure 10. The spectrum of the amorphous sample consists clearly of a magnetic hyperfine pattern and a paramagnetic one. The first component with broad lines and an effective field near 273 kG corresponds to amorphous Fe-B. The second component which is a quadrupole doublet at 85 K becomes magnetic at 4.2 K with an average hyperfine field 485 kG. The Mössbauer parameters of this spectral component are typical for small particles of α-Fe_2O_3. The spectrum of the crystalline sample can be analyzed as a superposition of three magnetic hyperfine patterns as shown by the solid line (Fig. 10b). The first component with narrow lines and an effective field 340 kG is of α-Fe. The other two spectral components have broad lines and an average hyperfine field of 490 kG. These magnetic components start to broaden at T > 4.2 K and finally resolve into a doublet at 300 K. The hyperfine parameters of this component are very similar to previously reported parameters of small particles of α-Fe_2O_3 [14]. The values of isomer shifts for Fe^{2+}, $Fe^{2.5+}$ are close to those in bulk Fe_3O_4 and FeO. An indirect experiment supported the presence of

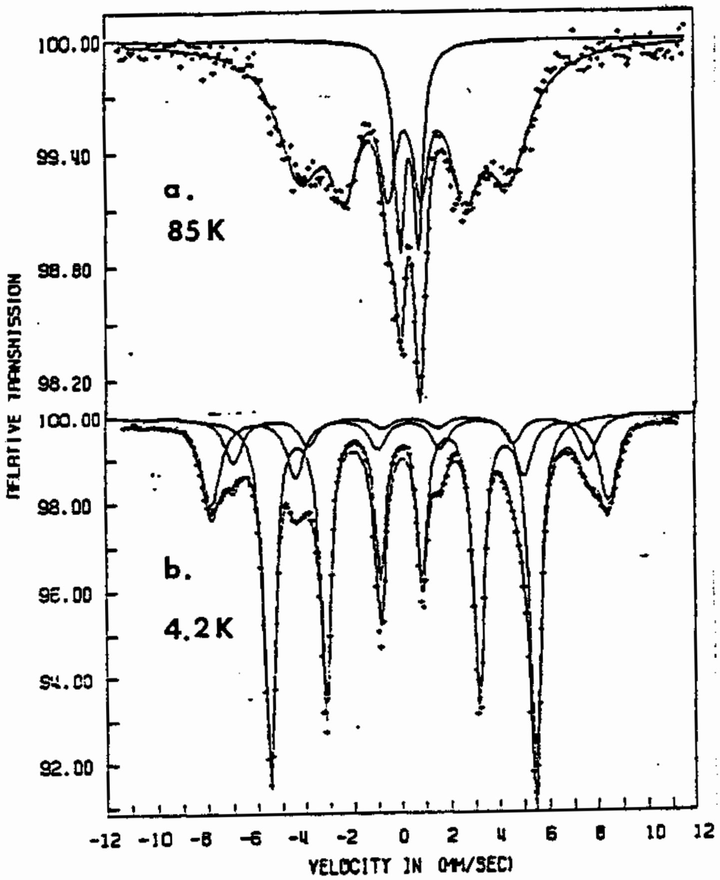

Figure 10. Mössbauer spectra for FeB samples (a) amorphous at 85 K, and (b) crystalline at 4.2 K.

an oxide coating around the Fe-B core. A sample was prepared by drying the as-made powder in a N_2 atmosphere inside a chamber. The sample was then split in two halves; the first was packed in a sample holder outside the chamber and the other one inside the chamber. The two samples were found to have different coercivities, 900 and 750 Oe, with the higher value obtained on the sample packed outside the chamber. Thus it may be speculated that the coercivity of the sample is mainly due to the surface oxide layers which coat the Fe-B core.

4. The "Shell-Core" Model

The structural, magnetic and Mössbauer data indicate a shell/core type of particle morphology. In Fe, Co and Ni particles, the core consists of metallic α-Fe, fcc Co and Ni respectively and the shell of the corresponding oxides ($Fe_3O_4/\gamma\text{-}Fe_2O_3$, CoO and NiO). In the Fe-B particles the core is an amorphous Fe-B matrix in the amorphous sample (B > 20 at.%) and bcc Fe(B) in the crystalline samples. The shell consists of $Fe_3O_4/\gamma\text{-}Fe_2O_3$. The shell/core model can explain adequately the magnetic hysteresis behavior of the particles and the size dependence of magnetization. In Fe particles, the Mössbauer data indicates a strong exchange interaction at the core/shell interface. Such exchange interaction at the core/shell interface could enhance the coercivity at 10 K. At temperatures greater than 40 K (crossover temperature in Figure 5) where the oxide shell becomes superparamagnetic, this exchange interaction between the superparamagnetic shell and the hard magnetic Fe core would make the whole particle magnetically soft, resulting in a strong temperature dependence of coercivity in smaller particles where the volume fraction of oxide is very large.

This model was further strengthened by the behavior of Fe/Ag samples where the amount of oxide on the particle surface was minimized [15]. This resulted (as expected) in a strong reduction of temperature dependence of coercivity; furthermore, the crossover among the coercivity vs temperature curves disappeared, as it is shown in Figure 7.

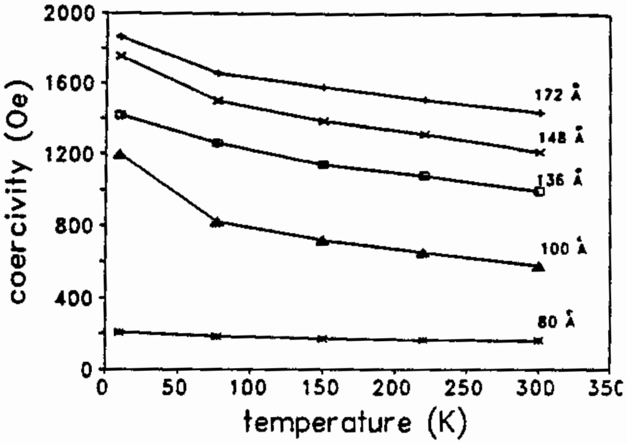

Figure 11. Reduced temperature dependence of coercivity in the case of Fe/Ag samples; the crossover temperature as in the case of passivated Fe samples is not present.

In Fe-B the size of the particles is much larger than the size of the Fe particles (by approximately a factor of 5) and therefore the effect of core/shell interface exchange interaction is not strong enough to affect the magnetic behavior of the particle as a whole. This results in a normal $H_c(T)$ behavior with a small increase in coercivity with decreasing temperature down to the Bloch temperature of the Fe-oxide where a stronger $H_c(T)$ dependence is observed.

As it was pointed earlier, the magnetization is usually decreased with decreasing particle size, because of dilution effects due to the lower magnetization of the oxides. However, the magnetization values below 90 emu/g can not be explained by the dilution hypothesis. In the past a similar effect was observed in fine Fe-oxide particles, where magnetization values as small as 30 emu/g were observed in γ-Fe_2O_3 [16]. The reduced magnetization values have been attributed to different effects. Berkowitz et al [16] explained the lower M_s by assuming the existence of a non-magnetic layer ("dead" layer) at the surface of the particles. Later Morrish et al [17] and Coey et al [18] claimed that the "dead" layer is due to surface spin canting. Recently this idea has been disputed, however, and Pankhurst [19] claimed that the lower magnetization values are due to non-saturation (of magnetization) effects because of the random distribution of small Fe-oxide particles with enhanced values of magnetocrystalline anisotropy. Research in this area is presently very active and the latest results suggest are that the low M_s values are due to bulk spin-canting in the whole particle [20].

5. Acknowledgments

This work has been supported by NSF CHE-9013930.

6. References

1. Matijevic E. (1989) 'Fine Particles: Science and Technology', MRS Bulletin XIV, 19.
2. Ozaki M. (1989) 'Prepration and Properties of Well-Define Particles', MRS Bulletin XIV, 35.

3. Sharrock M. P. and Bodnar R. E. (1989) 'Magnetic Materials For Recording: An Overview With Special Emphasis On Particles', J. Appl. Phys. 57, 3919.
4. Tasaki A., Takao M. and Tokunaga H. (1974) 'Magnetic Properties of Ferromagnetic Metal alloy Fine Particles prepared by evaporation in inert gases', Jap. J. Appl. Phys. 13, 27.
5. Oppegard A. L., Darnell F. I., Miller H. C. (1961) 'Magnetic properties of single domain iron and iron-cobalt particles prepared by borohydride reduction' J.Appl.Phys. 32, 3184.
6. Kim S. G. and Brock J. R. (1987) 'Growth of ferromagnetic particles from cation reduction by borohydride ions' J. Coll. and Interf. Sci. 116, 431.
7. Linderoth S., Morup S., Koch C. J. W., Wells S., Charles S. W., Van Wonterghem J. and Meagher A. (1988) 'Ultrafine particles of amorphous $Fe_{63}B_{38}$, A study of structural relaxation and crystallization', J. de Physique 49, c-1369.
8. Gangopadhyay S. and Hadjipanayis G. C. 'Magnetic properties of ultrafine particles', Submitted to Phys. Rev. B.
9. Kneller E. F., Luberosky F. E. (1963), 'Particle size dependence of coercivity and remanence of single domain particles', J. Appl. Phys. 34, 656.
10. Cullity B. D. (1972) Introduction to magnetic materials, Addison-Wesely Publishing Company, 347.
11. Papaefthymiou V., Kostikas A., Simopoulos A., Niarchos D., Gangopadhyay S., Hadjipanayis G. C., Sorensen C. M., and Klabunde K. J. (1990), 'Magnetic hysteresis and Mössbauer studies in ultrafine Fe particles', J. Appl. Phys. 67(9), 4487.
12. Haneda K. and Morrish A. H. (1978), 'Mössbauer study of Fe-oxide surface layers formed on small Fe particles', Surf. Sci. 77, 584.
13. Luborsky F. E. and Walter J. L. (1980) 'Preparation and properties of Fe-B-Si-C amorphous alloys', IEEE. Trans. Mag. mag-16, 572.
14. Van Der Kraan A. M.(1973) 'Mössbauer effect studies of surface ions of ultrafine-αFe2O3 particles' Phys. Stat. Sol. (a)1s, 215.
15. Gangopadhyay S., Hadjipanayis G. C., Shah S. I., Sorensen C. M., Klabunde K. J., Papaefthymiou V. and Kostikas A. (1991), 'Effect of oxide layer on the hysteresis behavior of fine Fe particles', J. Appl. Phys. 70.
16. Berkowitz A. E., Schuele W. J. and Flanders P. J. (1968) 'Influence of crystallite size on the magnetic properties of acicular γ-Fe_2O_3 particles', J. Appl. Phys. 39, 1261.
17. Morrish A. H., Haneda K. and Schurer P. J. (1976) 'Surface magnetic structure of small γ-Fe_2O_3 particles', J. Phys. Colloq. 37, C6-301.
18. Coey J. M. D. (1972), 'Noncollinear spin arrangement in ultrafine ferrimagnetic crystallites', Phys. Rev. Lett. 27, 1140.
19. Pankhurst Q. A. and Pollard R. J. (1991) 'Origin of spin-canting anomaly in small ferrimagnetic particles', Phys. Rev. Lett. 67, 248.
20. Parker F. T., Foster M. W., Margulies D. and Berkowitz A. E. (1991) 'Spin canting in γ-Fe_2O_3 particles', J. Appl. Phys. 69, 4505.